Optimal activation of Fc-mediated effector functions by influenza virus hemagglutinin antibodies requires two points of contact

Paul E. Leon[a,b], Wenqian He[a,b], Caitlin E. Mullarkey[a], Mark J. Bailey[a,b], Matthew S. Miller[c], Florian Krammer[a], Peter Palese[a,1], and Gene S. Tan[a,1]

[a]Department of Microbiology, Icahn School of Medicine at Mount Sinai, New York, NY 10029; [b]Graduate School of Biomedical Sciences, Icahn School of Medicine at Mount Sinai, New York, NY 10029; and [c]Department of Biochemistry and Biomedical Sciences, Institute of Infectious Diseases Research, McMaster Immunology Research Centre, McMaster University, Hamilton, ON, Canada L8S 4K1

Contributed by Peter Palese, August 15, 2016 (sent for review July 17, 2016; reviewed by Wendy Barclay, Maryna C. Eichelberger, and Anice C. Lowen)

Influenza virus strain-specific monoclonal antibodies (mAbs) provide protection independent of Fc gamma receptor (FcγR) engagement. In contrast, optimal in vivo protection achieved by broadly reactive mAbs requires Fc–FcγR engagement. Most strain-specific mAbs target the head domain of the viral hemagglutinin (HA), whereas broadly reactive mAbs typically recognize epitopes within the HA stalk. This observation has led to questions regarding the mechanism regulating the activation of Fc-dependent effector functions by broadly reactive antibodies. To dissect the molecular mechanism responsible for this dichotomy, we inserted the FLAG epitope into discrete locations on HAs. By characterizing the interactions of several FLAG-tagged HAs with a FLAG-specific antibody, we show that in addition to Fc–FcγR engagement mediated by the FLAG-specific antibody, a second intermolecular bridge between the receptor-binding region of the HA and sialic acid on effector cells is required for optimal activation. Inhibition of this second molecular bridge, through the use of an $F(ab')_2$ or the mutation of the sialic acid-binding site, renders the Fc–FcγR interaction unable to optimally activate effector cells. Our findings indicate that broadly reactive mAbs require two molecular contacts to possibly stabilize the immunologic synapse and potently induce antibody-dependent cell-mediated antiviral responses: (*i*) the interaction between the Fc of a mAb bound to HA with the FcγR of the effector cell and (*ii*) the interaction between the HA and its sialic acid receptor on the effector cell. This concept might be broadly applicable for protective antibody responses to viral pathogens that have suitable receptors on effector cells.

hemagglutinin | influenza virus | antibody-dependent cell-mediated immunity | broadly reactive antibodies | Fcγ receptor

Influenza remains a public health concern, causing significant morbidity and mortality worldwide (1). Despite the availability of vaccines, the protection provided by influenza immunization is typically strain-specific, and seasonal vaccines must be reformulated yearly to match circulating strains. There is a vital need to improve influenza virus vaccination strategies. In the movement toward the development of a new generation of vaccines, one promising approach is to focus the immune response to target the conserved regions of the virus (2).

The influenza virus hemagglutinin (HA), composed of a membrane distal globular head domain and a membrane proximal stalk region, plays a central role in both viral replication and the immune response elicited by influenza viruses. During influenza infection, HA mediates the initial attachment to *N*-acetylneuraminic (sialic) acid motifs ubiquitously expressed on cell surfaces and facilitates fusion of the viral and endosomal membranes (3, 4). Strain-specific antibodies induced by seasonal vaccines that target the globular head domain of the HA neutralize influenza viruses by preventing binding of the HA to its receptor sialic acid, which is ubiquitously present on host cells. In fact, the presence of these hemagglutination-inhibiting antibodies is widely accepted as a correlate of protection by regulatory agencies (5). However, because the globular head of the HA is antigenically more variable, antibodies that target the head and inhibit hemagglutination are limited in their capacity to neutralize divergent strains. In contrast, the stalk region is much more conserved, and antibodies elicited against conserved stalk epitopes have been shown to be broadly protective (6–13).

The ability to establish high titers of broadly neutralizing antibodies directed against the HA stalk is a critical component in developing a broad-spectrum universal influenza virus vaccine (14–18). However, the in vitro neutralizing activity of stalk-specific monoclonal antibodies (mAbs) is generally inferior to that of hemagglutination-inhibiting mAbs, and differences in their inhibitory concentrations can approach 2- to 3-log differences (19, 20). This disparity in vitro between head-specific and stalk-specific antibodies can be significantly reduced in vivo to approximately fivefold in passive transfer challenge studies (19, 21). Our recent findings demonstrate that broadly neutralizing HA stalk-specific antibodies rely on Fc–FcγR interactions that potently engage innate immune cells, which contributes to increased efficacy in vivo (19, 21).

The activity of innate immune cells, such as natural killer (NK) cells, neutrophils, macrophages, and dendritic cells, is regulated through a balance of activating and inhibitory signals received from an array of cell surface receptors that interact with cytokines

Significance

The mechanism of how antiviral antibodies induce Fc–FcγR effector functions remains to be fully elucidated. Although the ability to activate effector functions is attributed to antibody isotype, this does not fully address why identical isotypes have different capabilities to stimulate effector function. We show that antibodies that target the influenza virus hemagglutinin (HA) require a second intermolecular interaction to optimally activate effector cells. We demonstrate that the receptor-binding domain of the HA is required to bind to sialic acid expressed on the surface of effector cells to optimize effector cell activation. This finding provides a basic understanding of how an optimal antibody-dependent cell-mediated response against influenza virus is achieved and may allow for better vaccine design.

Author contributions: P.E.L., W.H., P.P., and G.S.T. designed research; P.E.L., W.H., C.E.M., M.J.B., and G.S.T. performed research; P.E.L., W.H., C.E.M., M.J.B., M.S.M., F.K., P.P., and G.S.T. analyzed data; and P.E.L., W.H., C.E.M., P.P., and G.S.T. wrote the paper.

Reviewers: W.B., Imperial College; M.C.E., Center for Biologics Evaluation and Research, Food and Drug Administration; and A.C.L., Emory University School of Medicine.

The authors declare no conflict of interest.

[1]To whom correspondence may be addressed. Email: peter.palese@mssm.edu or gene.tan@mssm.edu.

or target cells (22, 23). Pattern recognition receptors, such as Toll-like receptors, c-type lectin, and natural cytotoxic receptors (NCRs), are germ line-encoded cell surface receptors that allow for spontaneous activation of effector cells of the innate immune system (23–25). FcγRs, in contrast, are responsible for bridging the innate and adaptive responses by providing an interface between innate immune cells and antigen-specific antibodies. The ability of an Ig to activate Fc-mediated effector functions is dependent on its relative affinities for the activating and inhibitory FcγRs, whereby an activating/inhibitory ratio can be assigned for each antibody isotype (26–29). Whereas the IgG isotype may partially explain the ability of antibodies to induce Fc–FcγR-mediated effector functions, it does not address why antibodies with identical activating isotypes differ in their capacity to induce activation of innate immune cells (19, 21).

Here we attempted to determine whether there are additional cooperative factors between target and effector cells that may regulate the ability of an antibody to optimally activate effector functions. We constructed several influenza virus HAs with a FLAG tag inserted in-frame on the globular head domain or in the stalk region, to evaluate the role of epitope location in FcγR-mediated immunity. We found that an anti-FLAG mAb differentially activated FcγRs based on the position of the FLAG epitope within the HA molecule. We also observed that the receptor-binding region of the globular head domain plays a crucial role in FcγR-mediated activation. In summary, optimal activation of FcγR-mediated effector activity requires both Fc–FcγR engagement and the receptor-binding domain interacting with its cognate ligand.

Results

Characterization of FLAG-Tagged HAs. We previously demonstrated that broadly reactive anti-influenza mAbs can induce Fc–FcγR effector functions, whereas strain-specific mAbs do not (19, 21). To elucidate the mechanism by which antibody-dependent cell-mediated immunity and antibody-dependent cellular cytotoxicity (ADCC) are regulated, we generated peptide-tagged HAs to determine whether the location of an epitope within the HA plays a role. Recombinant HAs were generated by inserting the FLAG epitope (DYKDDDDK) in-frame into the HA of A/Puerto Rico/8/1934 virus (PR/8) (H1N1) at several positions within the HA: one in the globular head region (site 135; 135 FLAG-HA), three at the top of the stalk (sites 291, 298, and 313; 291 FLAG-HA, 298 FLAG-HA, and 313 FLAG-HA), or one at the base of the stalk region (site 366; 366 FLAG-HA) (Fig. 1*A*; insertion sites for the FLAG epitope indicated in red). The sialic acid-binding region marked by residues Y108, W166, H196, and L207 (indicated in green) is at the top of the globular head (Fig. 1*A*). The

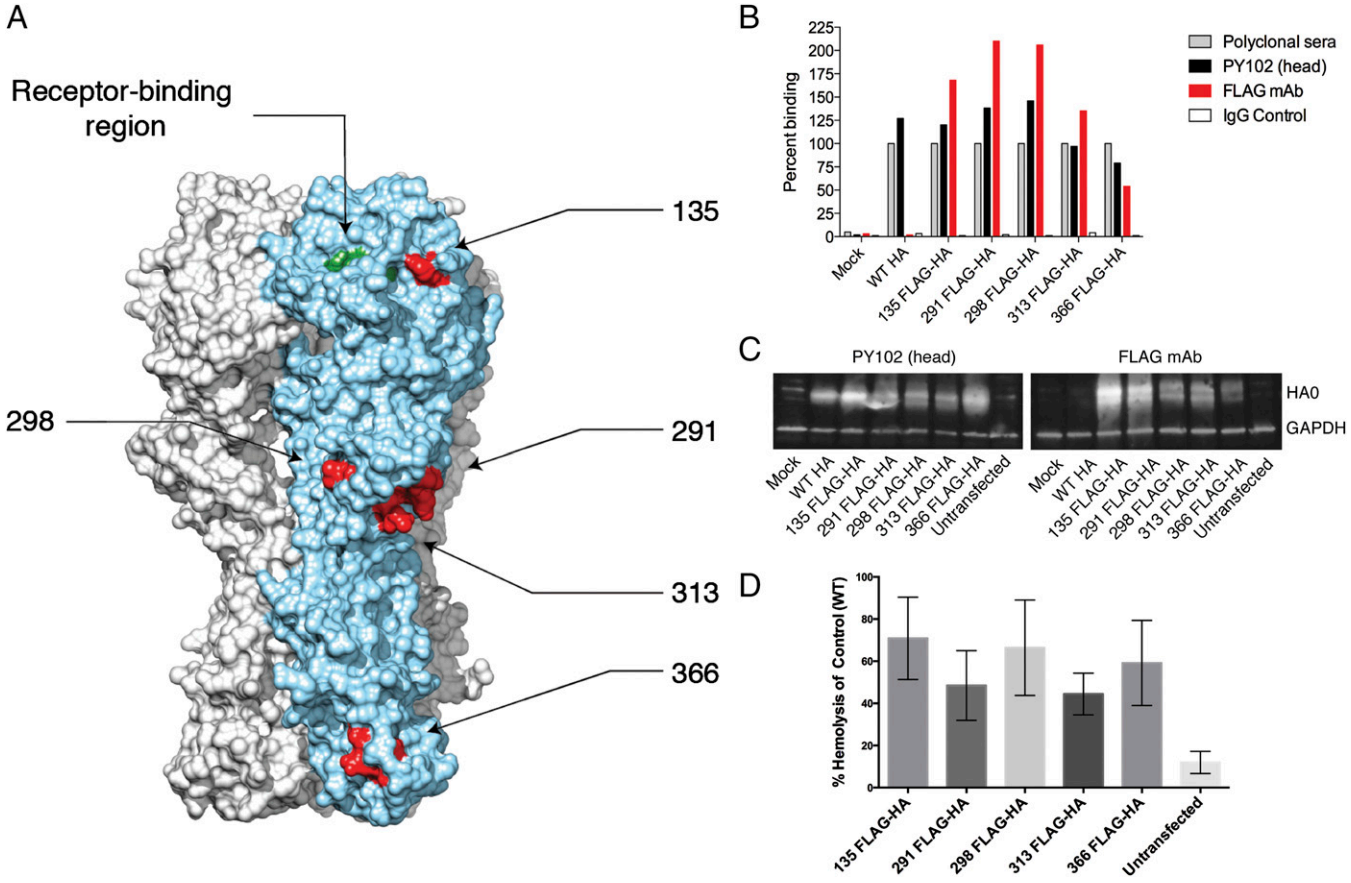

Fig. 1. Characterization of FLAG-tagged HAs. (*A*) The FLAG epitope (DYKDDDDK) was inserted in frame into PR/8 (H1N1) HA at site 135, 291, 298, 313, or 366 (residues indicated in red). The receptor-binding region represented by amino acids Y108, W166, H196, and L207 (indicated in green) resides on top of the globular head of the HA. (*B*) Cell surface expression of FLAG-tagged HAs was assessed via FACS analysis on transfected 293T cells using polyclonal sera, head-specific mAb PY102, an anti-FLAG mAb, or an IgG2a control (mAb XY102). Percent binding for each HA construct was normalized to polylconal sera against each respective HA. (*C*) Expression of the FLAG epitope of the tagged HAs was further confirmed by Western blot analysis of whole cell lysates from transfected 293T cells using mAb PY102 and an anti-FLAG mAb. GAPDH served as a loading control. (*D*) Binding of FLAG-tagged HAs to sialic acid motifs was assessed by a modified hemolysis assay. FLAG-tagged HA transfected cells were coincubated with a 0.5% solution of chicken RBCs for 1 h at 4 °C. Heme released from agglutinated transfected cells was quantified by absorbance (405 nm). Error bars represent SEM.

choice of the insertion sites was dictated by our previous plasticity analysis of the HA and exposed loops found on a crystallized structure (Protein Data Bank ID code IRU7), which demonstrated that these sites can tolerate insertions (30).

To evaluate the surface expression of FLAG-tagged glycoproteins, human embryonic kidney (HEK) 293T cells were transfected with a pDZ plasmid encoding 135 FLAG-HA, 291 FLAG-HA, 298 FLAG-HA, 313 FLAG-HA, 366 FLAG-HA, or the wild type (WT) PR/8 HA. Mock-transfected cells served as a negative control. At 16 h posttransfection (hpt), HEK 293T cells were harvested and cell surface expression was assessed using polyclonal sera, a head-specific mAb with hemagglutination-inhibiting activity (PY102) (31), or an anti-FLAG mAb by flow cytometry. As shown in Fig. 1*B*, polyclonal sera and the mAb PY102 recognized all recombinant FLAG-tagged HAs and the WT HA, whereas the anti-FLAG mAb bound only to HAs expressing the FLAG epitope.

To further assess the integrity of the FLAG epitope, lysates from transfected cells as described above were resolved on SDS/PAGE gels, and the epitopes of both mAb PY102 and FLAG were identified by Western blot analysis. Similar to the flow cytometry data, mAb PY102 recognized all recombinant HAs, whereas the anti-FLAG mAb bound only to FLAG-tagged HAs (Fig. 1*C*). An antibody to glyceraldehyde 3-phosphate dehydrogenase (GAPDH) served as a loading control. Taken together, these data demonstrate that insertion of an 8-aa peptide into the PR/8 HA did not substantially affect the proper folding of the influenza glycoprotein or the expression of the FLAG epitope as determined by surface expression and Western blot analysis.

To ensure that the insertion of the FLAG-tag epitope into the aforementioned residues of HA did not perturb binding of these HAs to sialic acid, we relied on a modified hemolysis assay. To this end, a 0.5% solution of chicken red blood cells (RBCs) was allowed to incubate with HEK 293T cells expressing FLAG-tagged constructs for 1 h at 4 °C to allow for HA binding. To trigger fusion of viral and cellular membranes, sodium citrate buffer (pH 5.2) was added, and the mixture was incubated for another 3 h at 37 °C. Once HA is bound to sialic acid on RBCs, acidification leads to a conformational change that initiates fusion and leads to RBC hemolysis. The amount of heme released in the supernatant is thus directly proportional to the virus–cell membrane fusion. Importantly, fusion activity is possible only when HA is bound to sialic acid (3, 4); therefore, any observed hemolysis activity serves as a proxy for sialic acid binding. All of the FLAG HAs displayed enhanced hemolysis activity (means ranging from 44% to 70% hemolysis compared with control; Fig. 1*D*) compared with the untransfected controls (12%). These data indicate that all of the FLAG-tagged HA constructs were capable of binding sialic acid.

Antibodies Bound to Epitopes Located in the Stalk Region Induce Antibody-Dependent Cell-Mediated Immunity. To model the activation of ADCC, we assessed the ability of a murine IgG2a anti-FLAG mAb to induce FcγR effector functions by targeting different FLAG-tagged HAs. HEK 293T cells were transfected with WT or FLAG-tagged HAs and at 16 hpt incubated with mAbs PY102 (strain-specific, IgG1), 6F12 (pan-H1, IgG2b) (19, 31), anti-FLAG, or an irrelevant Ig (IgG2a) control at a starting concentration of 10 μg/mL. After incubation with antibody, effector cells were added into the system, followed by incubation for another 6 h. Activation of antibody-dependent FcγR effector function was measured by luciferase activity under the transcriptional control of nuclear factor of activated T cells in a genetically modified Jurkat cell line stably expressing the murine FcγRIV (32). The anti-FLAG mAb weakly induced (fourfold) FcγR-mediated effector function when targeting an epitope adjacent to the receptor-binding site, 135 FLAG-HA, and did not induce the WT HA (Figs. 1*A* and 2 *A* and *B*). Remarkably, the anti-FLAG mAb induced activation of FcγR effector function by up to 8- to 13-fold only when targeting stalk-based epitopes (291 FLAG-HA, 298 FLAG-HA, 313 FLAG-HA, and 366 FLAG-HA) (Fig. 2 *C–F*). Of note, this is in stark contrast to our binding data, where FLAG-specific antibody bound to 135 FLAG-HA by roughly threefold higher than to 366 FLAG-HA as assessed by flow cytometry (Fig. 1*B*) and Western blot analysis (Fig. 1*C*), indicating that effector activation is not due to the expression level of the FLAG epitope. We speculate that an antibody binding to an epitope close to the receptor-binding site might not be able to induce optimal effector functions because it sterically hinders the interaction between the HA and sialic acid on the surface of the effector cell.

The broadly neutralizing mAb, 6F12, activated FcγRIV when targeting the WT HA or the 135 FLAG-HA (Fig. 2 *A* and *B*). Unsurprisingly, the strain-specific mAb PY102 or the isotype IgG2a control did not induce effector activity against any of the other HA constructs. Of note, given the location of the epitope insertion points for 291 FLAG-HA, 298 FLAG-HA, 313 FLAG-HA, and 366 FLAG-HA (Fig. 1*A*), which may alter the cognate epitope of a stalk-specific mAb (33), it is not surprising that 6F12 did not activate FcγR effector function against the FLAG epitopes found on the HA stalk region (Fig. 2 *C–F*). Here we show that the location of an epitope influences the ability of an antibody to trigger FcγR effector activity. Specifically, stalk-based membrane proximal epitopes have a greater capacity to induce antibody-dependent FcγR effector functions compared with epitopes adjacent to the sialic acid-binding site.

Blocking the Interaction Between the Receptor-Binding Region on the HA and Its Receptor Sialic Acid on the Effector Cell Prevents Antibody-Dependent FcγR Effector Activity. The inability of an epitope adjacent to the receptor-binding site to induce FcγR effector activity led us to postulate that the receptor-binding domain plays a key role in regulating effector cell induction. To test this, we used a head-specific $F(ab')_2$ to block the receptor-binding activity of the HA. First, HEK 293T cells were transfected with WT HA, and at 16 hpt, mAbs were coincubated with a constant amount (10 μg/mL) of a hemagglutination-inhibiting mAb (PY102) $F(ab')_2$ that targets the receptor-binding site. Modified Jurkat cells expressing murine FcγRIV to measure FcγR-mediated effector activity were then added into the system. As expected, a stalk-specific broadly neutralizing mAb (6F12) induced FcγR-mediated effector activity, whereas a strain-specific hemagglutination-inhibiting mAb (PY102) did not (Fig. 3*A*). The ability of 6F12 to induce FcγR-mediated effector activity was completely abolished in the presence of the $F(ab')_2$ of PY102, however, indicating that binding of HA to sialic acid on the effector cell is required for induction (Fig. 3*A*). Conversely, when the concentration of the stalk antibody (6F12; 10 μg/mL) was held constant and the $F(ab')_2$ PY102 was titrated out, induction of effector cell was increased in a dose-dependent manner (Fig. 3*B*).

To confirm that the addition of $F(ab')_2$ of PY102 into the system did not compete with 6F12 in binding to its epitope on the HA stalk, we performed a cell-based competition ELISA. In brief, a constant amount of a humanized [murine $F(ab')_2$ and human Fc] 6F12 (10 μg/mL) and a variable amount of PY102 $F(ab')_2$ (starting dilution of 10 μg/mL; diluted fourfold) were added onto WT HA-transfected HEK 293T cells, and an anti-human IgG-specific secondary antibody conjugated to horseradish peroxidase (HRP) was used to detect binding of the humanized 6F12. The humanized 6F12 alone bound equally well in the presence of either PY102 or control $F(ab')_2$ (Fig. 3*C*), indicating that binding of PY102 $F(ab')_2$ did not prevent 6F12 from binding to the stalk region. We confirmed that the $F(ab')_2$

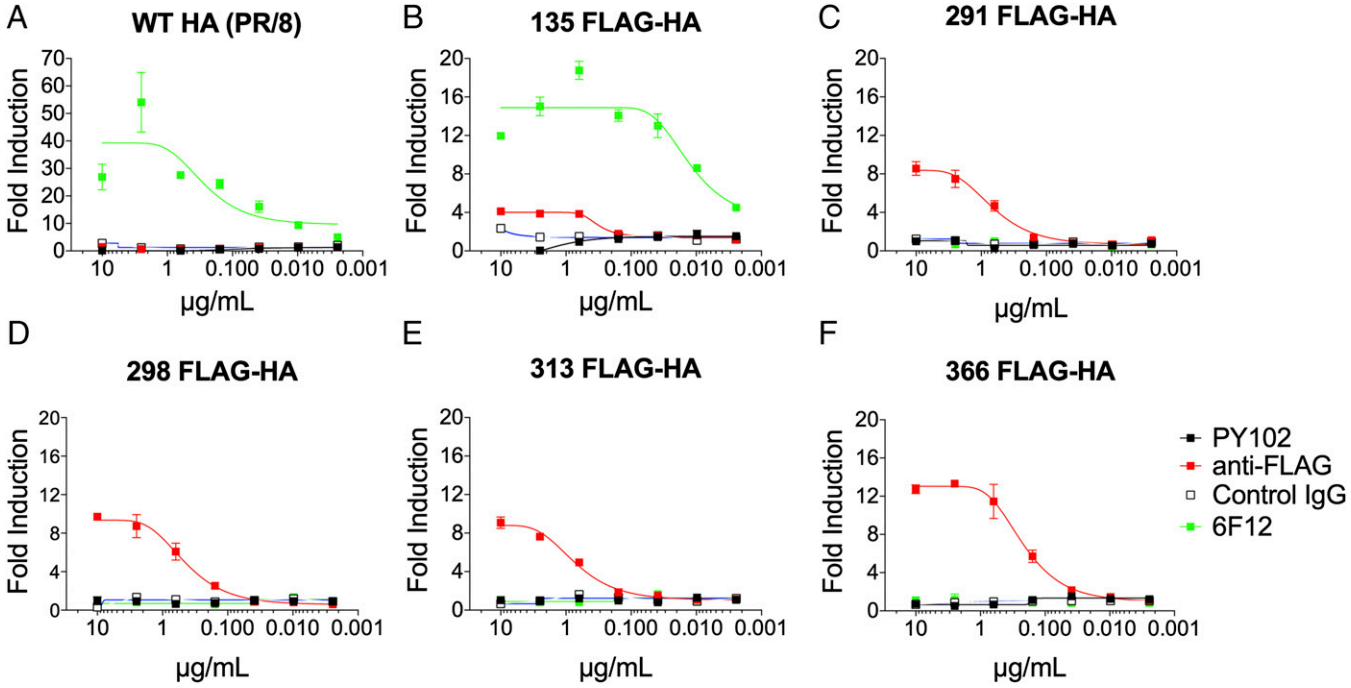

Fig. 2. A stalk-based FLAG epitope can induce FcγR-mediated effector function. To examine the role of epitope location on the induction of effector function, HEK 293T cells were transfected with WT HA (*A*), 135 FLAG-HA (*B*), 291 FLAG-HA (*C*), 298 FLAG-HA (*D*), 313 FLAG-HA (*E*), or 366 FLAG-HA (*F*). WT or FLAG-tagged HA-expressing HEK 293T cells were used as targets for measuring antibody-mediated effector function with a genetically modified Jurkat cell line expressing the murine FcRγIV with an inducible luciferase reporter gene. The mAb PY102 (IgG1) is a strain-specific antibody that recognizes the globular head of the HA of the PR/8 (H1N1) virus, and the mAb 6F12 (IgG2b) is a pan-H1 stalk-specific mAb. An H3-specific mAb, XY102 (IgG2a), served as a control IgG. The anti-FLAG mAb (IgG2a) is a commercially available antibody (Clontech). All mAbs were tested at a starting concentration of 10 µg/mL and were serially diluted fourfold. A nonlinear regression best-fit curve was generated for each dataset using GraphPad Prism 5. Error bars represent SEM. Results are from one of two independent experiments.

PY102 preparation did not contain any full-length IgG via Western blot analysis (Fig. 3*D*).

We previously demonstrated that the anti-FLAG mAb targeting the 366 FLAG-HA leads to the induction of effector function (Fig. 2*F*). Consistent with our data for 6F12 targeting WT HA (Fig. 3*A*), addition of the $F(ab')_2$ PY102 also effectively blocked the ability of an anti-FLAG mAb that targets a stalk-based epitope to induce effector function (Fig. 3*E*). Finally, we constructed an HA from the A/California/04/09 (H1) influenza A virus with a point mutation (tyrosine to phenylalanine at residue 108) in its receptor-binding site (Y108F HA), which was previously shown to affect sialic acid binding, to assess whether the HA mutant would affect activation by a stalk-specific antibody (34, 35). the ability of the stalk-specific mAb 6F12 to activate FcγRIV against Y108F HA was reduced by >75% compared with that against WT HA (Fig. 3*F*).

Taken together, the foregoing data indicate that optimal induction of FcγR-mediated effector activity requires a second molecular point of contact between the receptor-binding site on top of the HA globular domain and sialic acid motifs on the effector cell, in addition to the Fc–FcγR interaction. Moreover, effector functions mediated by a stalk mAb are diminished when this molecular link between the influenza HA and sialic acid motifs located on the effector cells is blocked.

Discussion

The precise mechanism by which broadly reactive influenza HA antibodies elicit the antiviral activity of innate immune leukocytes, such as macrophages, neutrophils, or NK cells, has not been fully characterized. Previous work has demonstrated that broadly neutralizing mAbs that target the influenza HA stalk require Fc–FcγR interactions for optimal protection in vivo, whereas strain-specific mAbs that bind to the receptor-binding pocket of the globular head do not (19, 21). Specifically, it was previously shown that immune complexes between HA and stalk-specific mAbs are superior in engaging FcγRs compared with immune complexes between HA and head-specific mAbs. However, an HA and head-specific mAb immune complex can activate effector function by engineering/increasing the affinity of the Fc for FcγRs. This observation indicates that (*i*) the Fc of head-specific mAbs are equally accessible as stalk-specific mAbs to engage FcγRs, and (*ii*) perhaps binding of certain epitopes (e.g., located on the globular head) may induce conformational changes that affect FcγR engagement.

To circumvent the potential confounding results posed by different epitopes and antibodies, we chose to focus on the role of the location of the epitope in inducing FcγR-mediated immunity. Toward this end, we inserted a peptide (FLAG epitope) in-frame into different sites of the influenza H1 HA: one on the head (135 FLAG-HA), three at the top of the stalk (291 FLAG-HA, 298 FLAG-HA, and 313 FLAG-HA), and one at the base of the stalk (366 FLAG-HA). This experimental system ensured that the epitope and the mAb were held constant, but allowed for the location of the epitope to vary. We confirmed the ability of these constructs to bind to sialic acid using a modified hemolysis assay in which viral fusion served as a proxy for sialic acid binding. The goal of these experiments was to verify sialic acid binding, not to evaluate the relative fusion abilities of these tagged HA constructs. We observed that an anti-FLAG mAb can induce effector cell activity when targeting stalk-based epitopes, but cannot induce such a response when bound to an epitope adjacent to the receptor-binding region of the globular head domain of HA. Remarkably, induction of Fc-mediated effector function by an anti-FLAG mAb targeting a stalk epitope was ablated by blocking the receptor-binding pocket

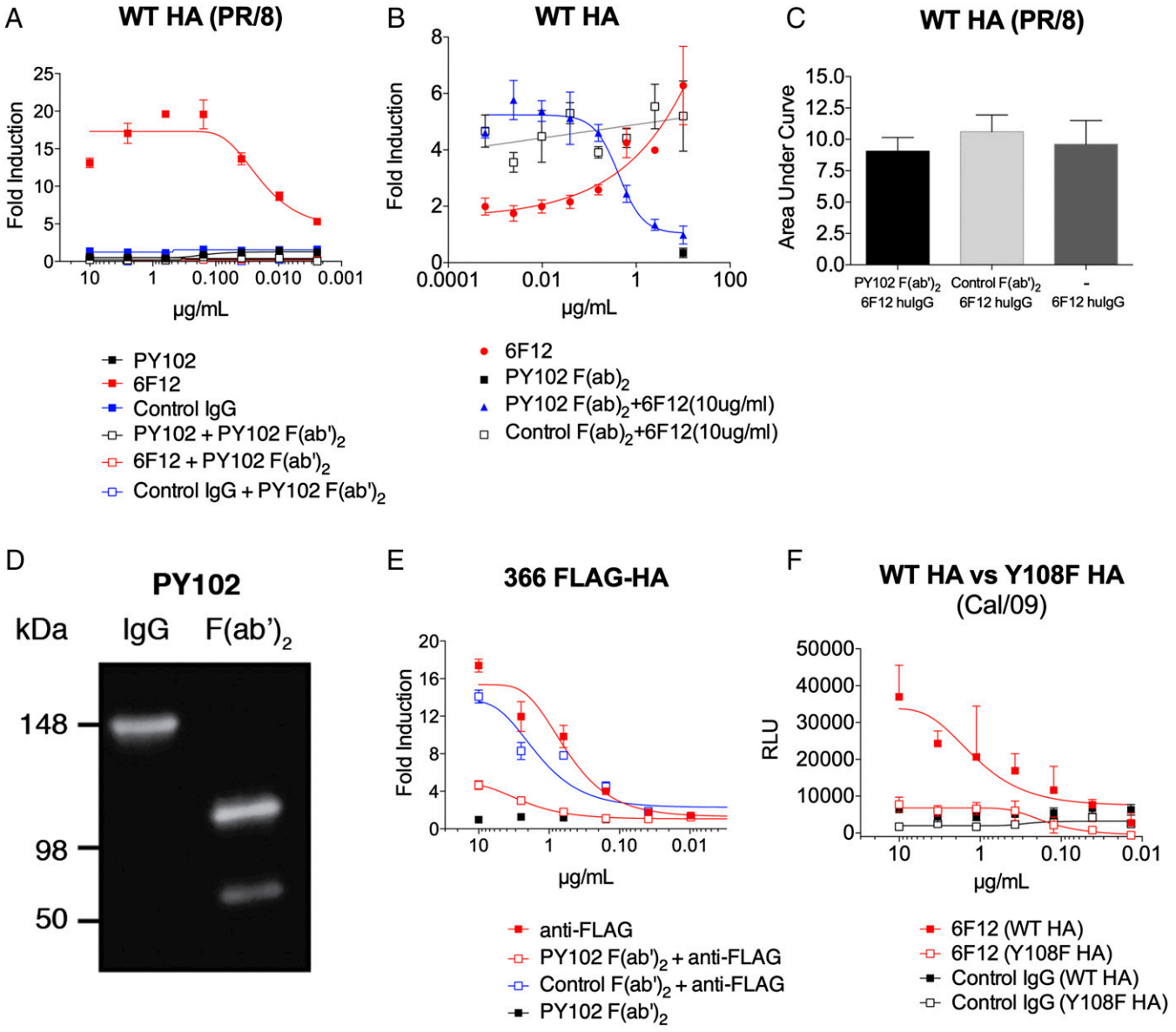

Fig. 3. Inhibition of HA binding to its sialic acid receptor prevents FcγR-mediated effector function induced by HA stalk mAbs. HEK 293T cells were transfected with WT HA (PR/8) (*A–C*), 366 FLAG-HA (*E*), WT HA (Cal/09) (*F*), or a mutant HA with a point mutation in the receptor binding site. Y108F HA (Cal/09) served as FcγR-mediated effector targets for the indicated mAbs. A genetically modified Jurkat cell line expressing the murine FcγRIV with an inducible luciferase reporter gene was used to determine the induction of antibody-mediated effector activity. (*A*) Induction of FcγR-mediated effector function by a stalk-specific mAb, 6F12, was inhibited by blocking the sialic acid-binding site of the globular head of HA with coincubation of a constant amount (10 μg/mL) of head-specific PY102 F(ab′)$_2$. (*B*) FcγR-mediated effector function by a stalk-specific mAb, 6F12 (10 μg/mL), was inhibited in a dose- dependent manner with the addition of a serial dilution of PY102 F(ab′)$_2$ (starting concentration of 10 μg/mL, diluted fourfold) (*C*) Coincubation of a constant amount (10 μg/mL) of humanized [murine F(ab′)$_2$, human Fc] 6F12 with variable amounts of PY102 or control F(ab′)$_2$ (starting concentration of 10 μg/mL, fourfold dilution) did not prevent 6F12 from binding to the stalk region in a cell-based ELISA. (*D*) Purified preparations (100 ng) of full-length and F(ab′)$_2$ of PY102 were resolved in an SDS/PAGE gel (in nonreducing conditions) and assessed by Western blot analysis. An anti-mouse F(ab′)$_2$-specific secondary antibody conjugated to HRP was used to visualized the antibody isoforms. (*E*) Induction of an anti-FLAG mAb against 366 FLAG-HA was also inhibited with a constant amount of PY102 F(ab′)$_2$ (10 μg/mL). (*F*) A stalk-specific mAb, 6F12, has reduced ability to induce effector activity against Y108F HA (Cal/09) compared with WT HA (Cal/09). Full-length mAbs in *A* and *E* were tested at a starting concentration of 10 μg/mL and were serially diluted fourfold, whereas the F(ab′)$_2$ in *A* and *E* were coincubated at a constant concentration of 10 μg/mL. The F(ab′)$_2$ in *B* was added at a starting dilution of 10 μg/mL and was diluted fourfold. An H3-specific mAb, XY102, was used as control IgG in *A* and *F*, and the control F(ab′)$_2$ in *B* and *E* was generated from a pan-H3 mAb, 9H10. The area under the curve in *C* was calculated using GraphPad Prism 5 from ELISA values read at 492 nm. A nonlinear regression best-fit curve was generated for each dataset using GraphPad Prism 5. RLU, relative luminescence units. Error bars represent SEM. Results are from one of two independent experiments.

with an F(ab′)$_2$ of a hemagglutination-inhibiting mAb (Fig. 3). Similarly, the ability of a broadly neutralizing stalk-specific mAb, 6F12, to activate effector functions also can be abolished using the bivalent F(ab′) (Fig. 3).

To further elucidate the role of the HA receptor-binding site in inducing effector activity, we generated an HA from A/California/04/09 (Cal/09) (H1) with a tyrosine-to-phenylalanine point mutation at residue 108 (Y108F HA). This mutation has previously been shown to have the greatest impact in lowering sialic acid binding activity (34, 35), although it is important to keep in mind that the receptor-binding domain is composed of several residues that contribute to receptor recognition, including W166,

H196, and L207 (35). Consistent with the results achieved using the bivalent F(ab′), we found that the Y108F Cal/09 HA decreased stalk antibody-mediated activation of effector cells by >75% compared with WT HA (Fig. 3*F*).

Here we describe a mechanism through which antibody-dependent cell-mediated immunity is regulated by two intermolecular interactions. The variability imposed by different epitopes and mAbs that may confound the interpretation of results was overcome by using an identical epitope and mAb for part of our studies. Focusing solely on the relationship between an epitope's location and its ability to induce effector activation, we demonstrate that sialic acid engagement by the HA receptor-binding domain is required for optimal activation of FcγR-mediated effector functions by HA stalk-specific antibodies. Specifically, our data show that the interaction between the receptor-binding domain on the influenza HA and sialic acid motifs on the effector cells provides a second contact point in addition to the antibody Fc–FcγR interaction to activate an effector cell (Fig. 4). In contrast, antibodies that target the receptor-binding pocket or adjacent residues do not induce or only weakly induce Fc-mediated effector functions because the second contact point between the receptor-binding pocket and sialic acid is sterically blocked (Fig. 4).

Viral HAs from pathogens such influenza virus and poxvirus (36, 37), as well as the HA-neuraminidase from Sendai virus and Newcastle disease virus, can bind to natural cytotoxic receptors, NKp46 and NKp44, and are able to activate NK cells independent of antibodies (38–40). In addition, HIV and herpes simplex virus also up-regulate the expression of other natural cytotoxic receptors (41, 42). Although the genetically modified Jurkat T cells used in this study might not express pattern recognition receptors, it is plausible that HA can bind to other cell surface receptors on the Jurkat T cells and contribute to antibody-mediated effector activation.

Nonetheless, our data help explain the apparent dichotomy between the disparate abilities of head- or stalk-specific antibodies to induce effector cell activity. We suggest that an anti-influenza antibody that does not interfere with the interaction between the receptor-binding site and sialic acid has the ability to induce FcγR-mediated effector function, which may include but is not limited to stalk-specific, non-HI active neutralizing head-specific or nonneutralizing antibodies (21, 43, 44). Although our data highlight the importance of this second point of contact, at present it is unclear whether HA binding to sialic acid activates an additional signaling pathway or facilitates stabilization of the immunologic synapse to prolong the interaction between an immune cell and the Fc region of an antibody.

Our work shed light on the molecular basis of how anti-influenza antibodies can engage the innate immune system to achieve optimal protection against influenza virus infection. Whereas the isotype of an antibody is an important factor for binding activating FcγRs (27–29), our studies clearly demonstrate that the location of an epitope on the influenza HA is critical in determining whether a second molecular bridge is available to fully engage the antiviral activity of an innate effector cell. We speculate that this second interaction required for optimal activation of Fc effector activity by a viral protein is not limited to the influenza virus HA. Other viral pathogens, such as HIV-1, rhinoviruses, and respiratory syncytial virus, also may induce optimal activation of effector cells through two molecular links: the Fc–FcγR interaction and a molecular bridge between a receptor-binding site on the viral protein and the receptor molecule on the effector cell. Indeed, numerous viral receptors have been found on effector cells. For example, the rhinovirus receptors, low-density lipoprotein and very-low-density lipoprotein, are found on macrophages (45–47). The respiratory syncytial virus receptor, CX3CR1 (48, 49), is found on intestinal macrophages, whereas CD81, an entry factor for hepatitis C virus, is also found on macrophages (50, 51). Finally, it is evident from previous studies that Fc–FcγR-mediated cellular immunity plays a major role in mounting an effective protective response toward bacterial pathogens (52, 53). Even in those circumstances, it is possible that a molecular bridge between the pathogen and the effector cell may enhance cell-mediated immunity.

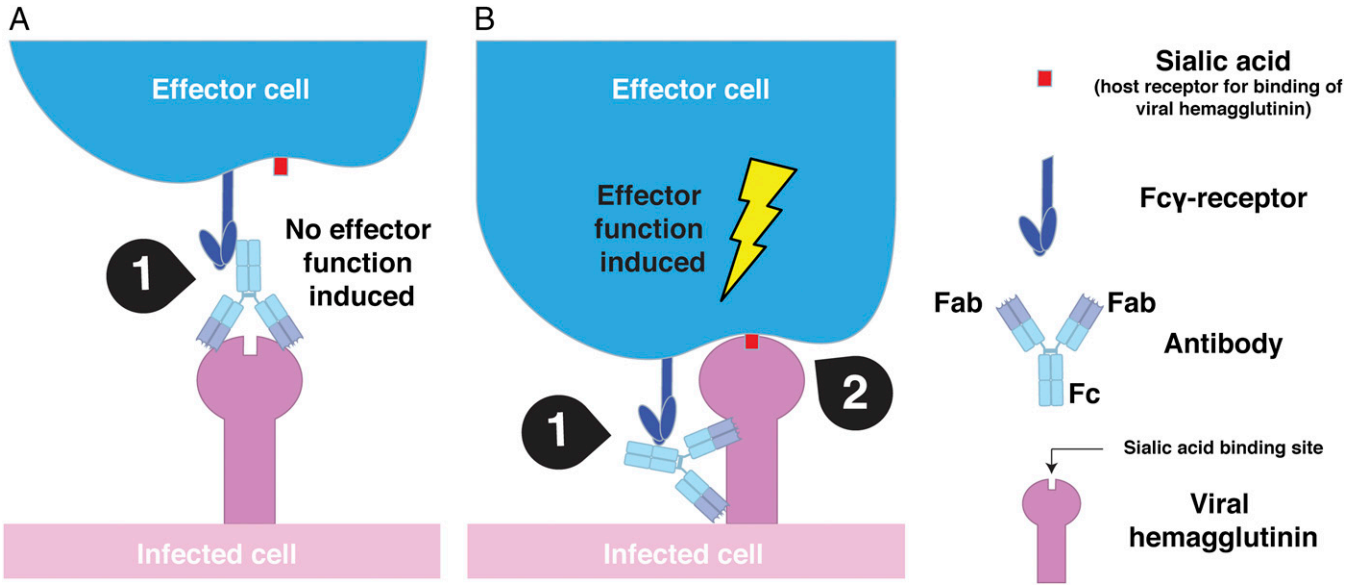

Fig. 4. Optimal activation of FcγR-mediated effector function requires two intermolecular contacts. (*A*) Classical hemagglutination-inhibiting antibodies that target the receptor-binding domain of the HA do not efficiently induce Fc-mediated effector functions because of steric hindrance of the receptor-binding site and subsequent loss of the second point of contact. Only one contact point between Fc and FcγR is established (1). (*B*) The interaction between the receptor-binding domain of the influenza virus HA and sialic acid motifs on the surface of effector cells (2) provides a second intermolecular bridge in addition to the Fc–FcγR interaction (1) and leads to optimal activation of an effector cell. The scenario described in *B* might possibly apply to any (viral) pathogen that has suitable receptors on effector cells.

Methods

Antibodies. The mAb with hemagglutination-inhibiting activity, PY102, specifically recognizes the globular head of the HA of PR/8 (H1N1) influenza A virus (31). The mAb XY102 recognizes the globular head of the HA of A/Hong Kong/1/1968 (H3) (54). The broadly neutralizing mAbs 6F12 (pan-H1) (7) and 9H10 (pan-H3) (8) that recognize the HA stalk have been described previously. The mAbs PY102, 6F12, XY102, and 9H10 were harvested from hybridomas and purified as described previously (7). The FLAG-specific mAb is a commercially available antibody (635691; Clontech). A humanized 6F12 was generated by subcloning the murine variable heavy chain and light chain sequences into a human pFUSE IgG1 and kappa expression vectors (Invivogen), respectively. The process of generating and purifying recombinant humanized mAb has been described previously (43, 44). All antibodies used were murine mAbs with an IgG2a isotype except for mAb 6F12, with an IgG2b isotype, and PY102, with an IgG1 subtype.

$F(ab')_2$ versions of mAb PY102 and 9H10 were generated using immobilized ficin and pepsin (Thermo Fisher Scientific), respectively. In brief, 1 mg of the full-length mAb PY102 (IgG1) and 9H10 (IgG2a) were incubated with immobilized ficin and pepsin, respectively, at 37 °C for 1 h to generate the $F(ab')_2$. The digested $F(ab')_2$ was then purified through a Protein A spin column [with the flow-through containing the $F(ab')_2$ saved] and quantified using a NanoDrop 2000 spectrophotometer (extinction coefficient factor of 1.4). The bivalent $F(ab')_2$ was assessed by SDS/PAGE in nonreducing conditions and detected with an anti-mouse $F(ab')_2$ antibody conjugated to HRP (1:10,000) by Western blot analysis.

Construction of FLAG-Tagged and Mutant HAs. The FLAG epitope (DYKDDDDK) was inserted in-frame into the HA of PR/8 influenza virus (H1N1) following residues 135, 291, 298, 313, or 366 (methionine, residue 1) using an overlapping PCR method. The coding regions of the FLAG-tagged HAs were subsequently subcloned into the ambisense expression plasmid pDZ (55). The HA of A/California/04/09 (H1) virus with a defective receptor-binding site (Y108F) was generated by mutating the tyrosine at site 108 (methionine, residue 1) into a phenylalanine and was subcloned into pDZ (34).

Evaluation of Cell-Surface Expression of FLAG-Tagged HAs by FACS. HEK 293T cells were transfected with a plasmid (pDZ) encoding WT PR/8 HA or FLAG-tagged HAs. At 24 hpt, cells were harvested and stained with primary antibodies (mouse polyclonal sera, mAb PY102 or FLAG) followed by an anti-mouse antibody conjugated to fluorescein isothiocyanate. Antibody binding to surface expressed HAs was then analyzed using FACS analysis, and data were processed using FlowJo software. Percent binding for each expressed HA was calculated by normalizing the data to polyclonal sera against WT HA. GraphPad Prism was used to generate the bar graph.

Evaluation of Antibody Binding to FLAG-Tagged HAs by Western Blot Analysis. HEK 293T cells were transfected with pDZ plasmids encoding wild-type PR/8 HA or FLAG-tagged HAs. Twenty-four hours post transfection, cells were lysed in radioimmunoprecipitation (RIPA) buffer (10 mM Tris·HCl/150 mM NaCl/1% Triton X-100/0.5% deoxycholate) for 10 min at 4 °C, then spun down at 12,000 × *g*, after which the lysate supernatants were collected. Lysates were resolved by 4–12% SDS/PAGE gels (Life Technologies). Gels were transferred to a nitrocellulose membrane and blocked with 5% nonfat milk in 1× PBS. Membranes were then stained with primary antibodies (mAb PY102, anti-FLAG mAb or a GAPDH antibody) (1:2,000) followed by an anti-mouse antibody conjugated to HRP (1:10,000).

ADCC. HEK 293T cells were seeded onto poly-D-lysine–coated 96-well white flat-bottom plates (Corning). At 24 h later, the cells were transfected with 100 ng per well of plasmid encoding WT, Y108F, or FLAG-tagged HA. At 16 hpt, the transfection medium was removed, and 25 μL of assay buffer (RPMI 1640 with 4% low-IgG FBS) was added to each well. Then mAbs were added in a volume of 25 μL at 30 μg/mL (for a final concentration of 10 μg/mL) and serially diluted fourfold in assay buffer (in triplicate). The bivalent PY102 $F(ab')$ was held constant at 10 μg/mL. Alternatively, the PY102 $F(ab')_2$ was added at a starting concentration of 10 μg/mL and diluted fourfold, and mAb 6F12 was held constant at 10 μg/mL. The antibodies were then incubated with the transfected cells for 30 min at 37 °C. Genetically modified Jurkat cells expressing the murine FcγRIV (32) with a luciferase reporter gene under the transcription control of nuclear factor-activated T cells were added at 7.5×10^4 cells at 25 μL per well, followed by incubation for another 6 h at 37 °C (Promega). Bio-Glo Luciferase assay reagent was added after 6 h, and luminescence was quantified using a plate reader. Fold induction, measured as relative luminescence units (RLUs), was calculated as follows: $(RLU_{induced} - RLU_{background})/(RLU_{uninduced} - RLU_{background})$. A nonlinear best-fitting curve was generated using GraphPad Prism 5 (56).

Cell-Based Competition ELISA. HEK 293T cells were seeded onto poly-D-lysine–coated 96-well tissue culture plates (BD Biosciences). At 24 h later, the cells were transfected with 100 ng of plasmid encoding WT HA. At 16 hpt, the cell monolayer was fixed with 100 μL of 3.7% paraformaldehyde for 10 min and then blocked with 100 μL of 5% nonfat milk/1× PBS for 30 min. PY102 $F(ab')_2$, control $F(ab')_2$, or no antibody was added at a starting concentration of 10 μg/mL and diluted fourfold, and a humanized [murine $F(ab')_2$ with human Fc] mAb 6F12 was held constant at 10 μg/mL. The primary antibody mixtures were incubated onto the cells for 30 min at room temperature, after which the plates were washed four times with 1× PBS/0.1% Tween (TPBS). An anti-human IgG-specific secondary antibody conjugated to HRP was then added (100 μL) at a dilution of 1:5,000, and the plates were incubated for another 30 min at room temperature. The plates were washed four times with TPBS, and 100 μL of *o*-phenylenediamine dihydrochloride (Sigmafast) substrate was added to develop the plates. The reaction was stopped with 80 μL of 3 M HCl, and the plates were read at 492 nm. Control $F(ab')_2$ was generated from a pan-H3 mAb, 9H10, as described above. A curve was generated, and the area under the curve was calculated using GraphPad Prism 5. Analyses of all groups were done in triplicate, except for the 6F12-only group, which were done in duplicate.

Generation of HA Molecular Model. The crystal structure of the HA of A/Puerto Rico/8/34 influenza virus (1RU7) was downloaded from the Protein Data Bank and used as a molecular model. The location of the FLAG peptide was indicated on the crystal structure using UCSF Chimera software (57).

Cell-Based Assay to Gauge Sialic Acid Binding. HEK 293T cells were transfected with pDZ plasmids encoding PR/8 or FLAG-tagged HAs in a 96-well plate as described previously. At 12–16 hpt, transfection media was removed from all wells and replaced with 50 μL of serum-free OptiPro (Gibco, Invitrogen). An equivalent volume of a 0.5% solution of chicken RBCs was added to the plate, followed by a 1-h incubation at 4 °C to allow for HA binding. After incubation, 100 μL of sodium citrate buffer (pH 5.2) was added and mixed well with the erythrocyte suspension to trigger hemolysis. The mixture was incubated for another 3 h at 37 °C. Plates were spun at 800 × *g* for 5 min to pellet unlysed RBCs, after which 100 μL of supernatant was transferred to new 96-well flat-bottom plates. To measure the heme of lysed RBCs that was released in the supernatant, the optical density of the supernatant was measured at 405 nm with a FilterMax F3 multimode microplate reader (Molecular Devices). The hemolysis titers are expressed as percent hemolysis of WT PR/8 as given by the following: $\{[A_{405}(\text{experimental}) - A_{405}(\text{RBCs only})]/[A_{405}(\text{WT PR/8}) - A_{405}(\text{RBCs only})]\} \times 100$.

ACKNOWLEDGMENTS. We thank Madhusudan Rajendran for excellent technical assistance in generating the Y108F A/California/4/09 HA. Funding for this study was provided by Center for Research on Influenza Pathogenesis Grant HHSN272201400008C (to P.P. and F.K.); National Institute of Allergy and Infectious Diseases Grants P01-AI097092 (to P.P.), U19-AI109946 (to P.P. and F.K.), and P01-AI097092-04S1 (to P.E.L.); and the Canadian Institutes of Health Research (M.S.M.)

1. World Health Organization (2014) *Fact Sheet 211: Influenza*. Available at: www.who.int/mediacentre/factsheets/fs211/en/. Accessed September 9, 2016.
2. Krammer F, Palese P, Steel J (2014) Advances in universal influenza virus vaccine design and antibody-mediated therapies based on conserved regions of the hemagglutinin. *Curr Top Microbiol Immunol* 386:301–321.
3. Bouvier NM, Palese P (2008) The biology of influenza viruses. *Vaccine* 26(Suppl 4):D49–D53.
4. Shaw ML, Palese P (2007) Orthomyxoviruses. *Fields Virology*, eds Knipe DM, Howley PM (Lippincott-Raven, Philadelphia, PA), 4th Ed.
5. Hobson D, Curry RL, Beare AS, Ward-Gardner A (1972) The role of serum haemagglutination-inhibiting antibody in protection against challenge infection with influenza A2 and B viruses. *J Hyg (Lond)* 70(4):767–777.
6. Okuno Y, Isegawa Y, Sasao F, Ueda S (1993) A common neutralizing epitope conserved between the hemagglutinins of influenza A virus H1 and H2 strains. *J Virol* 67(5):2552–2558.
7. Tan GS, et al. (2012) A pan-H1 anti-hemagglutinin monoclonal antibody with potent broad-spectrum efficacy in vivo. *J Virol* 86(11):6179–6188.
8. Tan GS, et al. (2014) Characterization of a broadly neutralizing monoclonal antibody that targets the fusion domain of group 2 influenza A virus hemagglutinin. *J Virol* 88(23):13580–13592.
9. Ekiert DC, et al. (2009) Antibody recognition of a highly conserved influenza virus epitope. *Science* 324(5924):246–251.
10. Ekiert DC, et al. (2011) A highly conserved neutralizing epitope on group 2 influenza A viruses. *Science* 333(6044):843–850.

11. Friesen RHE, et al. (2014) A common solution to group 2 influenza virus neutralization. *Proc Natl Acad Sci USA* 111(1):445–450.
12. Dreyfus C, et al. (2012) Highly conserved protective epitopes on influenza B viruses. *Science* 337(6100):1343–1348.
13. Wang TT, et al. (2010) Broadly protective monoclonal antibodies against H3 influenza viruses following sequential immunization with different hemagglutinins. *PLoS Pathog* 6(2):e1000796.
14. Krammer F, Pica N, Hai R, Margine I, Palese P (2013) Chimeric hemagglutinin influenza virus vaccine constructs elicit broadly protective stalk-specific antibodies. *J Virol* 87(12):6542–6550.
15. Yassine HM, et al. (2015) Hemagglutinin-stem nanoparticles generate heterosubtypic influenza protection. *Nat Med* 21(9):1065–1070.
16. Steel J, et al. (2010) Influenza virus vaccine based on the conserved hemagglutinin stalk domain. *MBio* 1(1):e00018-10.
17. Impagliazzo A, et al. (2015) A stable trimeric influenza hemagglutinin stem as a broadly protective immunogen. *Science* 349(6254):1301–1306.
18. Wohlbold TJ, et al. (2015) Vaccination with soluble headless hemagglutinin protects mice from challenge with divergent influenza viruses. *Vaccine* 33(29):3314–3321.
19. DiLillo DJ, Tan GS, Palese P, Ravetch JV (2014) Broadly neutralizing hemagglutinin stalk-specific antibodies require FcγR interactions for protection against influenza virus in vivo. *Nat Med* 20(2):143–151.
20. He W, et al. (2015) Broadly neutralizing anti-influenza virus antibodies: Enhancement of neutralizing potency in polyclonal mixtures and IgA backbones. *J Virol* 89(7): 3610–3618.
21. DiLillo DJ, Palese P, Wilson PC, Ravetch JV (2016) Broadly neutralizing anti-influenza antibodies require Fc receptor engagement for in vivo protection. *J Clin Invest* 126(2): 605–610.
22. Nimmerjahn F, Gordan S, Lux A (2015) FcγR-dependent mechanisms of cytotoxic, agonistic, and neutralizing antibody activities. *Trends Immunol* 36(6):325–336.
23. Porgador A (2005) Natural cytotoxicity receptors: Pattern recognition and involvement of carbohydrates. *ScientificWorldJournal* 5:151–154.
24. Moretta A, et al. (2001) Activating receptors and coreceptors involved in human natural killer cell-mediated cytolysis. *Annu Rev Immunol* 19:197–223.
25. Kruse PH, Matta J, Ugolini S, Vivier E (2013) Natural cytotoxicity receptors and their ligands. *Immunol Cell Biol* 92(3):221–229.
26. Stewart R, Hammond SA, Oberst M, Wilkinson RW (2014) The role of Fc gamma receptors in the activity of immunomodulatory antibodies for cancer. *J Immunother Cancer* 2:29.
27. Nimmerjahn F, Ravetch JV (2006) Fcgamma receptors: Old friends and new family members. *Immunity* 24(1):19–28.
28. Nimmerjahn F, Ravetch JV (2007) Fc-receptors as regulators of immunity. *Adv Immunol* 96:179–204.
29. DiLillo DJ, Ravetch JV (2015) Fc-receptor interactions regulate both cytotoxic and immunomodulatory therapeutic antibody effector functions. *Cancer Immunol Res* 3(7):704–713.
30. Heaton NS, Sachs D, Chen CJ (2013) Genome-wide mutagenesis of influenza virus reveals unique plasticity of the hemagglutinin and NS1 proteins. *Proc Natl Acad Sci USA* 110(50):20248–20253.
31. Reale MA, et al. (1986) Characterization of monoclonal antibodies specific for sequential influenza A/PR/8/34 virus variants. *J Immunol* 137(4):1352–1358.
32. Nimmerjahn F, Bruhns P, Horiuchi K, Ravetch JV (2005) FcgammaRIV: A novel FcR with distinct IgG subclass specificity. *Immunity* 23(1):41–51.
33. Tran EEH, et al. (2016) Cryo-electron microscopy structures of chimeric hemagglutinin displayed on a universal influenza vaccine candidate. *MBio* 7(2):e00257.
34. Whittle JRR, et al. (2014) Flow cytometry reveals that H5N1 vaccination elicits cross-reactive stem-directed antibodies from multiple Ig heavy-chain lineages. *J Virol* 88(8): 4047–4057.
35. Martín J, et al. (1998) Studies of the binding properties of influenza hemagglutinin receptor-site mutants. *Virology* 241(1):101–111.
36. Mandelboim O, et al. (2001) Recognition of haemagglutinins on virus-infected cells by NKp46 activates lysis by human NK cells. *Nature* 409(6823):1055–1060.
37. Jarahian M, et al. (2011) Modulation of NKp30- and NKp46-mediated natural killer cell responses by poxviral hemagglutinin. *PLoS Pathog* 7(8):e1002195.
38. Arnon TI, et al. (2001) Recognition of viral hemagglutinins by NKp44 but not by NKp30. *Eur J Immunol* 31(9):2680–2689.
39. Gazit R, et al. (2006) Lethal influenza infection in the absence of the natural killer cell receptor gene Ncr1. *Nat Immunol* 7(5):517–523.
40. Jarahian M, et al. (2009) Activation of natural killer cells by newcastle disease virus hemagglutinin-neuraminidase. *J Virol* 83(16):8108–8121.
41. Chisholm SE, Howard K, Gómez MV, Reyburn HT (2007) Expression of ICP0 is sufficient to trigger natural killer cell recognition of herpes simplex virus-infected cells by natural cytotoxicity receptors. *J Infect Dis* 195(8):1160–1168.
42. Vieillard V, Strominger JL, Debré P (2005) NK cytotoxicity against $CD4^+$ T cells during HIV-1 infection: A gp41 peptide induces the expression of an NKp44 ligand. *Proc Natl Acad Sci USA* 102(31):10981–10986.
43. Tan GS, et al. (2016) Broadly-reactive neutralizing and non-neutralizing antibodies directed against the H7 influenza virus hemagglutinin reveal divergent mechanisms of protection. *PLoS Pathog* 12(4):e1005578.
44. Henry Dunand CJ, et al. (2016) Both neutralizing and non-neutralizing human h7n9 influenza vaccine-induced monoclonal antibodies confer protection. *Cell Host Microbe* 19(6):800–813.
45. Rankl C, et al. (2008) Multiple receptors involved in human rhinovirus attachment to live cells. *Proc Natl Acad Sci USA* 105(46):17778–17783.
46. Neumann E, Moser R, Snyers L, Blaas D, Hewat EA (2003) A cellular receptor of human rhinovirus type 2, the very-low-density lipoprotein receptor, binds to two neighboring proteins of the viral capsid. *J Virol* 77(15):8504–8511.
47. Herijgers N, Van Eck M, Groot PH, Hoogerbrugge PM, Van Berkel TJ (2000) Low density lipoprotein receptor of macrophages facilitates atherosclerotic lesion formation in C57Bl/6 mice. *Arterioscler Thromb Vasc Biol* 20(8):1961–1967.
48. Johnson SM, et al. (2015) Respiratory syncytial virus uses CX3CR1 as a receptor on primary human airway epithelial cultures. *PLoS Pathog* 11(12):e1005318.
49. Medina-Contreras O, et al. (2011) CX3CR1 regulates intestinal macrophage homeostasis, bacterial translocation, and colitogenic Th17 responses in mice. *J Clin Invest* 121(12):4787–4795.
50. Evans MJ, et al. (2007) Claudin-1 is a hepatitis C virus co-receptor required for a late step in entry. *Nature* 446(7137):801–805.
51. Tippett E, Cameron PU, Marsh M, Crowe SM (2013) Characterization of tetraspanins CD9, CD53, CD63, and CD81 in monocytes and macrophages in HIV-1 infection. *J Leukoc Biol* 93(6):913–920.
52. Joos C, et al. (2010) Clinical protection from falciparum malaria correlates with neutrophil respiratory bursts induced by merozoites opsonized with human serum antibodies. *PLoS One* 5(3):e9871.
53. Kato N, et al. (2009) The E-selectin ligand basigin/CD147 is responsible for neutrophil recruitment in renal ischemia/reperfusion. *J Am Soc Nephrol* 20(7):1565–1576.
54. Moran TM, et al. (1987) Characterization of variable-region genes and shared cross-reactive idiotypes of antibodies specific for antigens of various influenza viruses. *Viral Immunol* 1(1):1–12.
55. Martínez-Sobrido L, García-Sastre A (2010) Generation of recombinant influenza virus from plasmid DNA. *J Vis Exp* (42):2057.
56. Cheng ZJ, et al. (2014) Development of a robust reporter-based ADCC assay with frozen, thaw-and-use cells to measure Fc effector function of therapeutic antibodies. *J Immunol Methods* 414(C):69–81.
57. Pettersen EF, et al. (2004) UCSF Chimera: A visualization system for exploratory research and analysis. *J Comput Chem* 25(13):1605–1612.